Modeling of Cavities Detection in The Tree Stem Section Using Radar Vector Network Analyzer (VNA) Elaborating Radon Transform

Aldi Rivaldi Dwinanda, Bambang Setia Nugroho, and Aloysius Adya Pramudita[*]

School of Electrical Engineering, Telkom University, Bandung, 40287, Indonesia

[*]pramuditaadya@telkomuniversity.ac.id

Abstract

Trees are one of the most useful plants for life on earth. However, trees can be harmful due to cavities in the stem sections. Rapid detection is needed to prevent several losses that may arise due to fallen trees. This research identified a hollow and non-hollow tree stem section of flamboyant tree with a sub-surface detection radar system. The sub surface detection radar system was modeled using a Vector Network Analyzer (VNA) connected to a Vivaldi antenna. VNA emitted electromagnetic waves to the tree stem section and subsequently propagated and penetrated hollow tree stem section. The propagation wave met the boundary plane between the wood and the cavity which reflected the electromagnetic waves. The reflected wave was caught by antenna and was display by the VNA as S-Parameter. This research used a Vivaldi antenna with a working frequency of 1 GHz – 10 GHz and a VNA with working frequency 300KHz - 8GHz. The difference in the amplitude of the signal could be seen from the results of cavity measurements made at one point. By implementing circular scanning method with inverse radon transformation, this research could identify a 19 cm diameter wood with a hole of 6 cm and 9.5 cm diameter filled with water, respectively. It was observed that the optimal detection was obtained by placing object between the antennas. This research has signified the application of radar modeled with VNA for detecting the cavities in tree stem section.

1. Introduction

Trees are one of the most useful plants for life on earth. One of its main benefits is being able to act as a filter to keep the air clean. However, trees can be harmful due to cavities in the stem sections. There are more than 3500 trees in the city of Bandung have been pruned and 33 others felled in anticipation of falling and taking casualties. Precise detection to determine the loss of tree stem section is necessary to prevent several losses that may arise due to fallen trees.

Ground Penetrating Radar (GPR) is a geophysical inspection technique used for investigations below the ground surface without destroying it. The working principle of the GPR system is based on the emission of electromagnetic pulse waves (EM) towards the investigated target [1]. This electromagnetic signal is reflected after entering the boundary between one field and another. This reflected signal is captured by the receiver [2].

The GPR system is also used on tree stem section as a method for detecting cavity or what is known as a surface detection radar. Electromagnetic waves propagate and penetrate the cavity of tree trunk subsequently the propagation meets the boundary between the wood and the cavity. This situation allows the reflection of electromagnetic waves.

In the previous research [3], experiments were carried out to detect cavities in tree stem section with the GPR system. The GPR system is modeled using a Vector Network Analyzer (VNA) to determine its performance in detecting voids. The reflected wave was caught by antenna and was displayed by the VNA as S-Parameter. However, the diameter of the tree trunk in this research was too small so it was difficult to identify and the measurement on a straight line was used in previous research.

In this research, experiments were carried out to detect cavities in tree stem section with a larger

diameter using a VNA radar system for a more accurate analysis of the identification process of porosity. The inverse radon transformation was used to display the image results from scanning measurements.

2. Research Method

In modern radar, there are transducers or sophisticated computer systems that not only detect the target and determine the target range but can also track, identify, image, and classify the target while minimizing unwanted interference such as echoes from the environment (clutter) and jamming [4].

2.1 Ground Penetrating Radar

Ground Penetrating Radar (GPR) is a geophysical inspection technique used for investigations below the ground surface without destroying it. The working principle of the GPR system is based on the emission of electromagnetic pulse waves towards the investigated target [1,2]. The frequency range of the VNA used in this experiment was 300 kHz to 8 GHz as previously used in Ref [3,17].

In radar systems, microwaves are emitted continuously in all directions by the transmitter. The object hit by this wave reflects it and the reflection wave is captured by the receiver and displayed by the radar screen [5,17].

When the reflection occurs at the boundary between two different mediums, the modeling of the VNA radar system in detecting cavities in tree stem section gives visible results. The wave propagation across a medium is reflected if it passes through a different medium. It is characterized by different values of relative permittivity (ε_r) and relative permeability (μ_r). In this model, two media with different permittivity (air and wood) were used.

Fig. 1 illustrates the arrangement of the medium contained in this model. The relative permittivity is influenced by the frequency and anisotropic direction [6]. The relative permittivity of dry wood is usually between 2 and 3.5. However, at the same time the permittivity can undergo significant changes as wood can contain more than 50% water compared to its total mass [7]. The density of wood affects its hygroscopic, shrinkage, strength, acoustic and electrical properties, and other properties [17]. Meanwhile, water has a relative permittivity of 80 [8].

2.2 Radar Modeling Using a Vector Network Analyzer (VNA)

The VNA has a transmitter (T_x) and a receiver (R_x) port that produces S-parameters with symbols S_{11}, S_{12}, S_{21}, and S_{22} [9]. S_{11} and S_{22} are the input and output reflection coefficients on port 1 and port 2, respectively. While S_{21} and S_{12} represent the forward and reverse transmission coefficients, respectively [9].
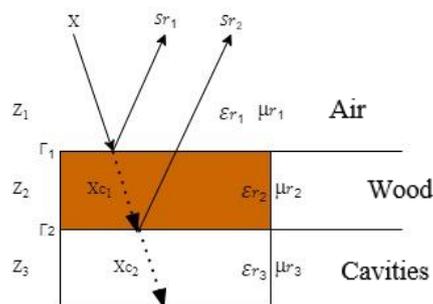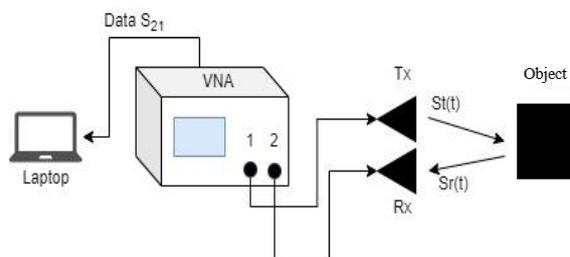

Fig. 1. Wave reflection process

Fig. 2. Radar modelling using a VNA

This model consists of two antennas connected by a VNA port. The VNA is set to take S_{21} measurements with a frequency range that matches the radar system. The S_{21} data represents the transfer function between the send signal and the received signal [10,19,20]. This data is subsequently sent to the computer to carry out the reconstruction process from the received signal.

The steps for modeling the radar were discussed in Ref. [10]. First, the required equipment is prepared as shown in Fig 2. Several functions are set in VNA including frequency range, measured data sample, complex data format, and S_{21} measurement. The S_{21} data are red on a computer or laptop and the Fast Fourier Transform (FFT) sequence of S_{21} is arranged as a transfer function which will be written as $S_{21}[k]$.

The transmission signal ($S_t[n]$) based is sequenced on the radar system and is converted to the frequency domain using Fast Fourier Transform (FFT) which is later written as $S_t[k]$. The convolution process between the transmission signal and the transfer function is performed to get the received signal. The multiplication process in the frequency domain between $S_t[k]$ and $S_{21}[k]$ and the inverse FFT are further performed. Other computational processes can be performed in the computational domain such as mixing, filtering, or other detection methods using Matlab [11,12].

2.3 Scanning Method

Scanning methods can be divided into three types, which ar A-Scan, B-Scan, and C-Scan [13]. Fig. 3 illustrates the scanning methods.
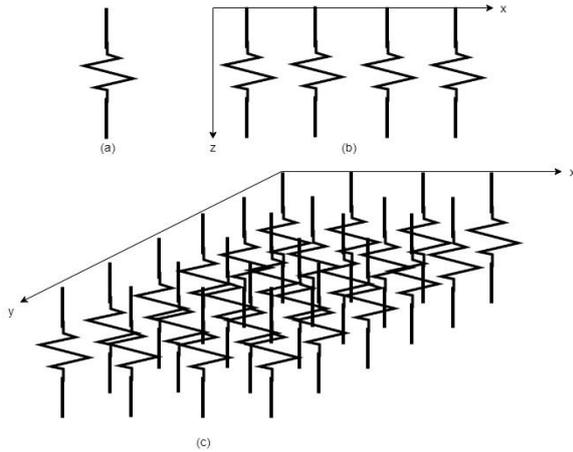
Fig. 3. (a) a-scan, (b) b-scan, and (c) c-scan

2.4 Radon Transformation

Tomography is a method of imaging the inside of an object. Imaging data is obtained from the total value of transmission, emission, or reflection by objects from various projection angles [14]. Radon transformation represents the image as a collection of one-dimensional signals resulting from the projection of the image at various orientation angles [15].

In the Matlab image processing toolbox, the radon transformation can be performed by calling the function:

$$[R, xp] = \text{radon}(\text{I}, \text{theta}) \qquad (1)$$

R represents the result of the Radon transformation of the original image I with the theta orientation range and the wide range of the projection area at the xp transformation coordinates [16].

2.5 Inverse Radon Transformation

Inverse radon transformation is the reconstruction of the radon transformation results into the initial data as before being transformed [2]. The inverse transformation of radon from the projection g(s,θ) R(f), -∞<s<∞,0≤θ≤ is formulated as follows:
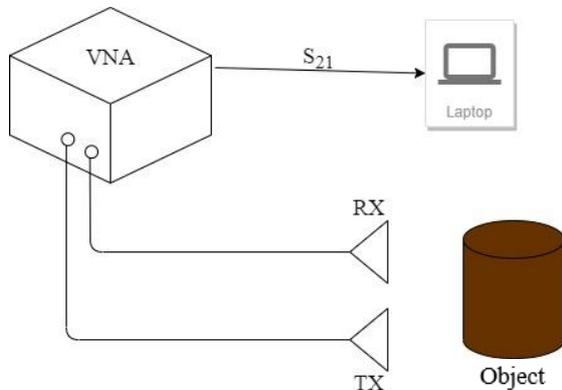

Fig. 4. VNA radar modeling

$$f(x,y) = \frac{1}{2\pi^2} \int_0^\pi \int_{-\infty}^\infty - \frac{[(\partial g/\partial s)(s,\theta)]}{x\cos\theta + y\sin\theta - s} ds d\theta \qquad (2)$$

Meanwhile, the inverse operation of the radon transformation can be written by calling a function. This function performs two operations, namely: unblurring and reverse projection. The functions are as follows:

$$I = i\text{radon}(\text{R}, 2) \qquad (3)$$

3. Design of Experiment

3.1 Radar Modeling

This experiment modeling radar using VNA as shown in Fig 4. Port 1 is used as a transmitter and port 2 as a receiver so that the S-parameter used is S_{21}. The format used for data retrieval is a polar format (R+jX). The value obtained is processed by the Matlab application. The frequency range used in VNA is 300KHz - 8 GHz with sweep mode as the mode used for data retrieval with a total data retrieval of 501 points.

3.2 Object Modeling and Detection Scheme

The objects of this experiments were 3 tree stem section with cavities and 2 tree stem section without cavities as shown in Fig. 5. The tree stem section with their diameters of 19.5 cm and height of 25 cm had 2 unnatural cavities with diameters of 9.5 cm and 6 cm (Fig. 5 (a)). The tree stem section with a diameter of 40 cm and height of 42 cm had a natural cavity with diameters of 2 cm (Fig. 5 (b)).

Fig. 6 shown the detection method. The detection in scheme I is done by placing two antennas parallel in front of the object and the detection method in scheme II is done by placing the object between two antennas that are facing each other

3.3 Signal Processing Method

In Fig. 7 there are several steps in signal processing including the modeling the radar using VNA and data collection S_{21}. In this section, the signal emitted by the VNA is reflected and received by the receiver antenna in the form of a data series in the frequency domain. The series is the number of data samples used. The sample data of this signal was stored on the VNA in a polar format. This data was subsequently transferred to a laptop for processing with Matlab.

Next, the signal reconstruction. It serves to convert the pulse signal into information data obtained from the form of the S_{21} data arrangement. This information data is subsequently displayed with the inverse transformation of radon and analyzed for its characteristics from the shape of the influence signal from wood with cavity and without cavity so that conclusions can be drawn.
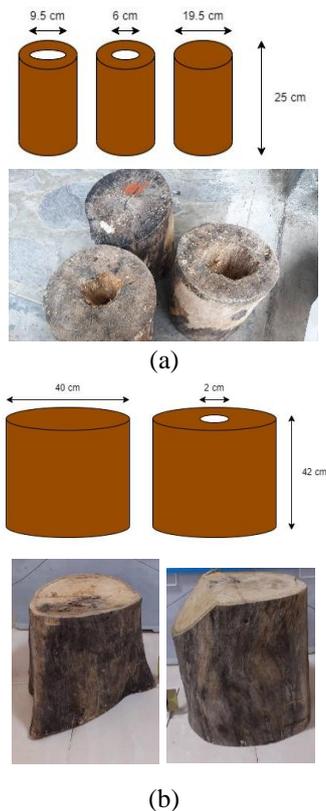
(a)

(b)

Fig. 5. Object modeling (a) unnatural cavities and (b) natural cavities
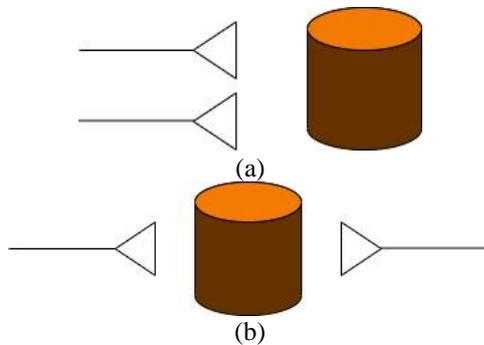

(a)

(b)

Fig. 6. Detection (a) scheme I and (b) scheme II

3.5 Data Processing Methods with Matlab

In Fig. 8, there are several steps in processing data with Matlab. First, the creation of source code. Making this source code by looking at the reference from the VNA radar modeling signal processing. Next, the S_{21} data obtained from the VNA was entered into Matlab. Subsequently, the S_{21} data series was arranged into an FFT series in the frequency domain.

The transmit pulse S_t was generated and subsequently converted into a discrete vector $S_t(n)$ with many S_{21} data, namely 501 points. This process is called discretization. Next, FFT will be calculated from $S_t(n)$. This FFT result is multiplied by the FFT of S_{21}. This process is called convolution. Subsequently determine the signal received by S_r using IFFT or
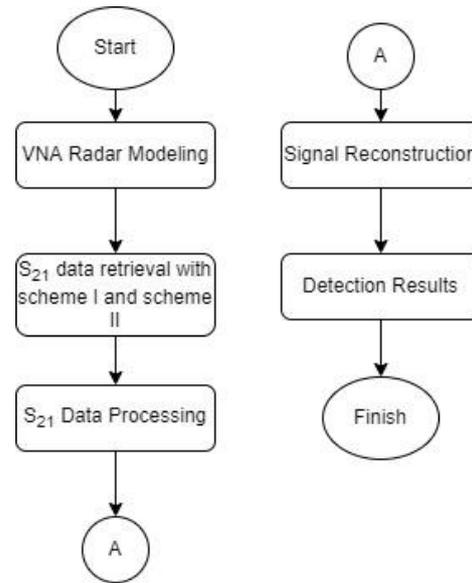

Fig. 7. Signal processing flow chart

(Inverse Fast Fourier Transform). This aims to determine the shift in the position of the reflected signal that occurs due to wave propagation through different media.

The signal that has been reconstructed into the time domain is filtered in the form of a signal in the form of a monocycle pulse with the aim of clarifying the reflections of the signal received by the antenna for easy analysis. This signal will be displayed using A-Scan for one point.

Subsequently, at many points, the received signals are organized into a data matrix. Furthermore, the image of this matrix will be displayed using the inverse radon transformation. It aims to simplify the analysis process by looking at the initial form of this image projection. After that, corrections are made to certain data series to clarify only the part where there are reflections on two different mediums, namely the cavities in the tree stem section.

Subsequently the image is compared between wood with cavity and without cavity if there is no difference subsequently add S_{21} data or remodel the object. If there are differences, subsequently proceed with analysis and conclusions. To remodel the object, researcher made larger cavities and added plastic filled with water with the aim of detecting cavities in the stem section to be seen more clearly.

4. Result and Discussion

4.1 Measurement Results of Tree Stem section with Natural Cavities

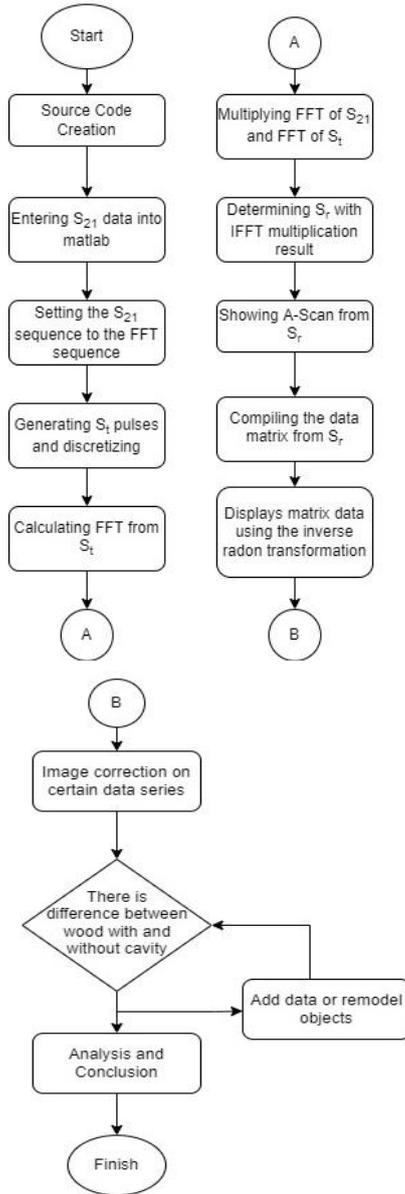In wood without cavity, the antenna-to-bark distance varies from 7.5 cm to 8.5 cm. While in wood
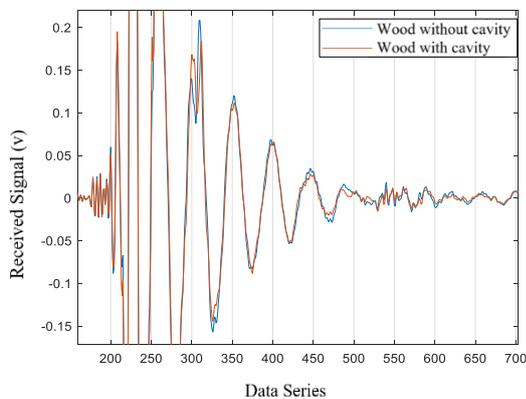
Fig. 8. Data processing flow chart

Fig. 9. The results of a-scan detection I on wood

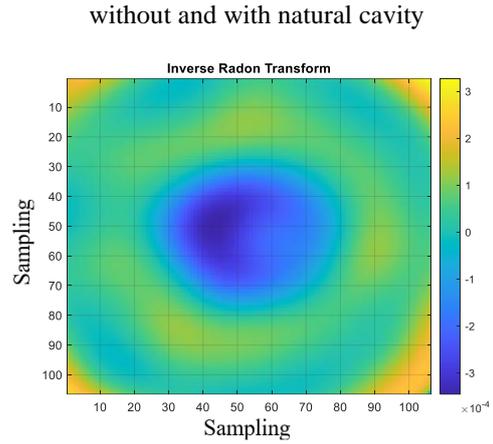without and with natural cavity

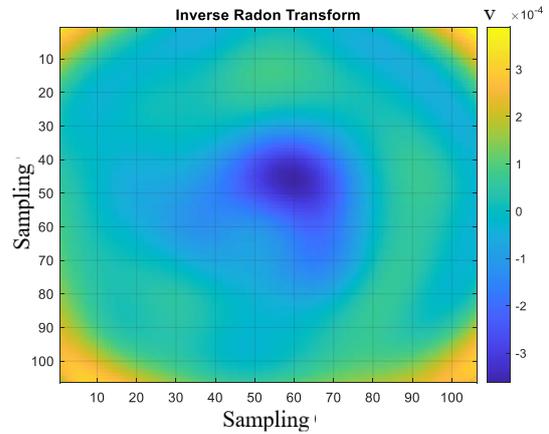Fig. 10. Result of inverse radon scheme I on natural wood without cavity

Fig. 11. Result of inverse radon scheme I on natural wood with cavity

with cavity, it varies from 8.5 cm to 9.5 cm. The distance from the antenna to the cavity also varies between 25.5 cm to 27.5 cm. This is because the shape of the wood was not perfectly round, and the position of the cavity is not located at the center of the wood. The cavity in this wood is 2 cm in diameter.

Measurements in scheme I are carried out by placing two antennas vertically parallel with 2 cm between the antennas on objects with natural cavity. This antenna is placed at 27.5 cm from the center of the object and 3.5 cm from the floor.

From the results of the detection scheme, I as in Fig. 9, the difference in signal in wood without cavity and wood with cavity can be seen in the 300-400 data series. The signal received in wood with cavity is greater than in wood without cavity.

The second measurement is carried out by circular scanning on wood with and without cavity. Measurements were made every ten degrees so that 36 points were produced. The X and Y-Axis show the data series or sampling of the data taken. In Fig. 10, it can be seen that the blue color depicts a small-received

33

v

signal due to the absence of a detected cavity so that there is no medium displacement.

Fig. 11 shows the results of the inverse radon transformation for wood with cavity after making corrections to the data series. At coordinates (50.60) the light blue color illustrates the received signal is greater than wood without cavity.

Fig. 12 shows the results of the detection scheme II. The signal received in wood with cavity is greater than in wood without cavity and can be seen in the data series 400-500.

The second measurement is carried out by circular scanning on wood with and without cavity. The X and Y-Axis show the data series or sampling of the data taken. In Fig. 13, the blue color depicts a small-received signal due to the absence of a detected cavity so that there is no medium displacement. The light blue color illustrates the received signal is greater than that of wood without cavity. Based on Fig. 14, wood without cavity and wood with cavity cannot be distinguished.
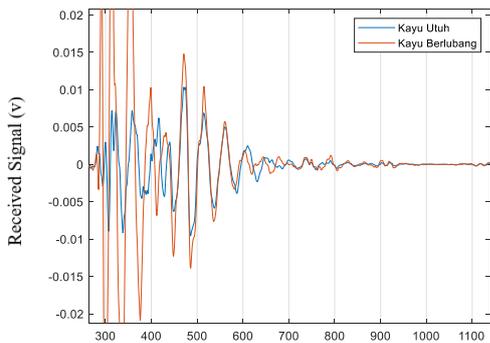

Fig. 12. The results of a-scan detection II on wood without and with natural cavity
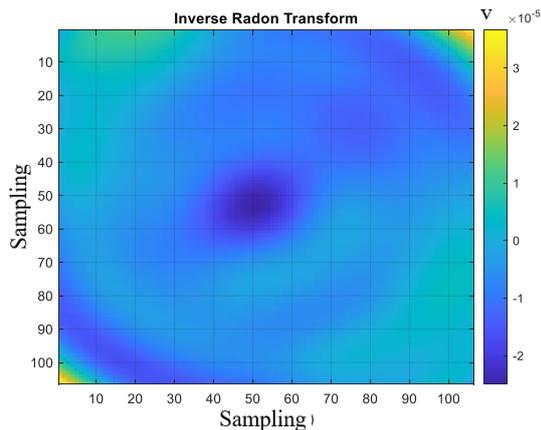

Fig. 13. Result of inverse radon scheme II on natural wood without cavity
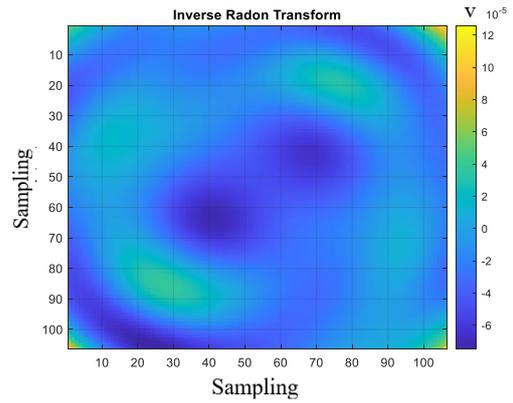

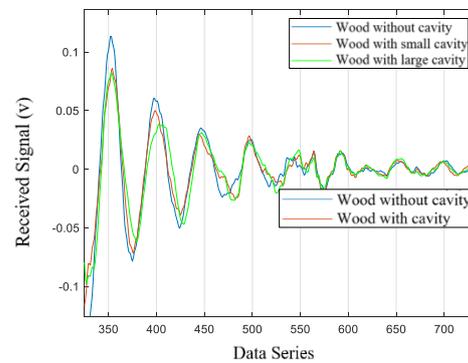Fig. 14. Result of inverse radon scheme II on natural wood with cavity

Fig. 15. The results of a-scan detection I on wood without and with unnatural cavity

4.2 Measurement Results of Tree Stem section with Unnatural Cavities

This measurement is carried out on each object of the tree stem section with and without cavity. Antenna settings are adjusted according to each scheme. Researcher made larger cavities and added plastic filled with water with the aim of detecting cavities in the stem section to be seen more clearly. Tree stem section have a relative permittivity of between two and three depending on the water content, while water has a relative permittivity of 81 and has a high conductivity.

Measurements in scheme I are carried out by placing two antennas vertically parallel with 2 cm between the antennas on objects with unnatural cavity. This antenna is placed at 14.5 cm from the center of the object and 6 cm from the floor.

The detection scheme I (Fig. 15) results 300-500 difference data series. The signal received in wood without cavity is greater than in wood with cavity.
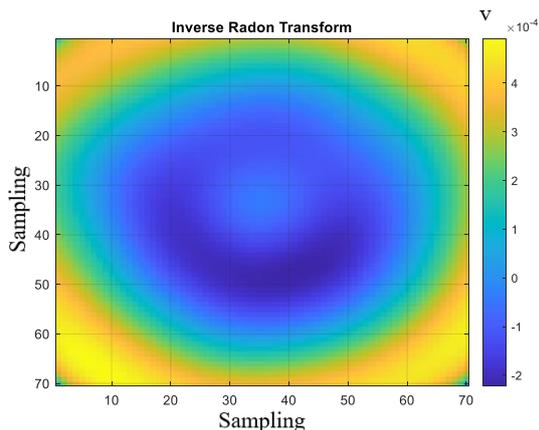
Fig. 16. Result of inverse radon scheme I on unnatural wood without cavity
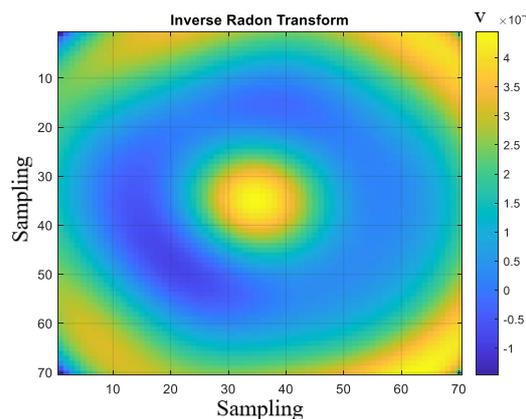

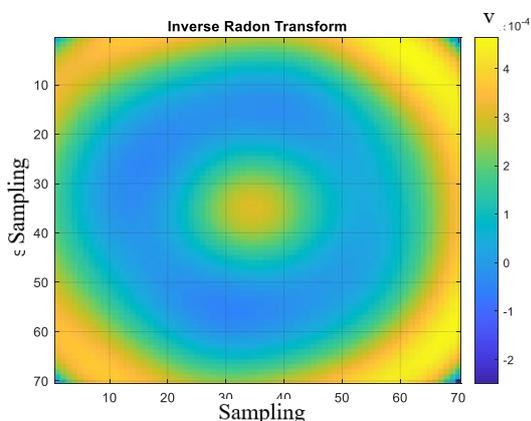Fig. 18. Result of inverse radon scheme I on unnatural wood with large cavity

Fig. 17. Result of inverse radon scheme I on unnatural wood with small cavity
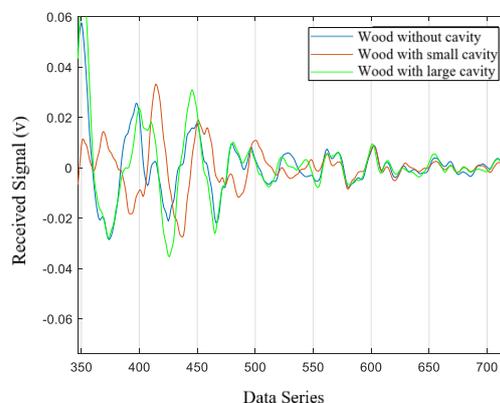

Fig. 19. The results of a-scan detection ii on wood without and with unnatural cavity

The second measurement is carried out by circular scanning on wood with and without cavity. Measurements were made every ten degrees so that 36 points were produced. The X and Y-Axis show the data series or sampling of the data taken.

It can be seen in Fig. 16 that the blue color depicts a small-received signal due to the absence of a detected cavity so that there is no medium displacement. The results of this scan are different from the results of wood without cavity.

The difference lies in the yellow color in the center of the image, namely the coordinates (35,35). This indicates a small cavity has been detected.

Fig. 17 results of inverse radon schema I on wood with unnatural small cavity. Around the coordinates (30,30), (30,40), (40,30), and (40,40) there is a yellow color that is not too dense. In the object, the small cavity has a diameter of 6 cm and is located at the center point of the stem section.

The yellow color illustrates that the received signal is larger because of the detected cavity resulting in the displacement of the medium.

Around the coordinates (30,30), (30,40), (40,30), and (40,40) there is a dense yellow color. In the object, the large cavity has a diameter of 9.5 cm and is located at the center point of the stem section.

The yellow area indicates the detected cavity. The yellow color illustrates that the received signal is larger because of the detected holes resulting in the displacement of the medium. This is in accordance with the theory of waves across the medium.

Measurement in scheme II is done by placing two antennas facing each other on an object with unnatural cavity. This antenna is placed at 14.5 cm from the center of the object and 12 cm from the floor.

From the results of the detection scheme II as shown in Fig. 19 the difference can be seen in the data series 400-500. The received signal is greater in wood with large cavity than wood with small cavity and wood without cavity.

The second measurement is carried out by circular scanning on wood with and without cavity. Measurements were made every ten degrees so that 36 points were produced. The X and Y-Axis show the data series or sampling of the data taken.
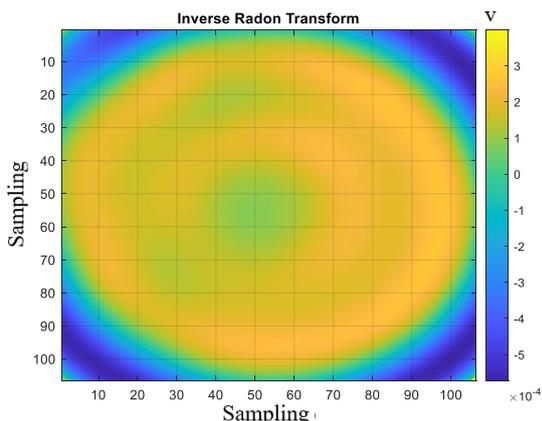
Fig. 20. Result of inverse radon scheme II on unnatural wood without cavity
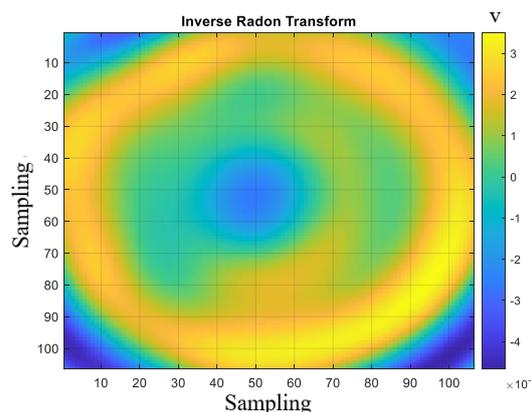

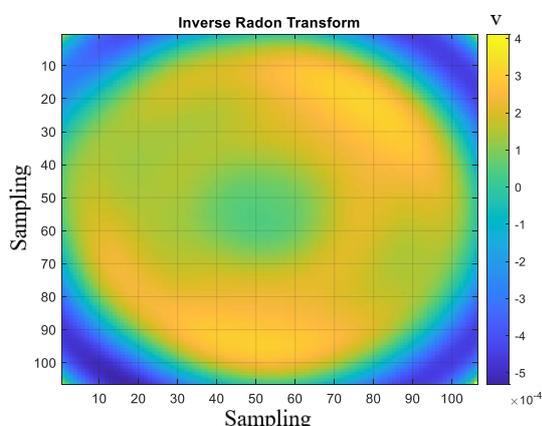Fig. 22. Result of inverse radon scheme II on unnatural wood with large cavity

Fig. 21. Result of inverse radon scheme II on unnatural wood with small cavity

Fig. 20 shows the results of the inverse radon transformation for wood without cavity after making corrections to the data series. The yellow color illustrates the large-received signal as a result of the absence of a detected cavity so that no medium displacement occurs.

The results in Fig. 21 are different from the results of wood without cavity. The difference lies in the less yellow concentration on the upper left, namely at the coordinates (30.30) and the lower right, namely at the coordinates (90.70). This indicates the detection of a small cavity.

Around the central coordinate, namely (50,50) there is a green color with a mixture of blue. In the object, the small cavity has a diameter of 6 cm and is located at the center point of the stem section. The turquoise color indicates that the received signal is smaller because of the detected cavity resulting in the displacement of the medium.

The results in Fig. 22 are different from the results of wood with small cavity. The difference lies in the density of the yellow color which turns into a greenish color in almost all parts that indicates a large cavity. Around the center coordinate (50,50) there is a darker

blue color than wood with small cavity. In the object, the large cavity has a diameter of 9.5 cm and is located at the center point of the stem section.

It can be seen that the blue- and turquoise-colored areas indicate the detected cavity. The blue color illustrates the received signal is smaller because of the detected cavity resulting in the displacement of the medium. This is in accordance with the theory of waves across the medium.

The water transmission coefficient is smaller than the wood transmission coefficient, so cavity filled with water are marked in blue and turquoise. This is caused by the high conductivity of water.

The results of the inverse radon transformation in the opposite scheme can also be analyzed better because there is a difference in size between the large and small cavity. This is different from parallel schemes where the difference lies in the magnitude or smallness of the received signal.

5.   Conclusions

This experiment has detected the cavities of tree stem section with relatively large difference on permittivity and conductivity. The inverse radon transformation can display and analyze the images more easily. Perforated wood has a different color density in the hollow part. Data retrieval is easier to analyze when the object was placed between two antennas.

References

[1]   A. M. Alani et al, The Use of Ground Penetrating Radar and Microwave Tomography for the Detection of Decay and Cavities in Tree Trunks *Remote Sensing*, 11(18) (2019)

[2]   R. Perciso, Introduction to Ground Penetrating Radar, The Institute of Electrical and Electronics Engineers, Inc., Hoboken, New Jersey (2014)

[3]   A. D. Pratiwi, Metode Indetifikasi Rongga pada Batang Kayu dengan Menggunakan Ground

Penetrating Radar (GPR), Universitas Telkom, Bandung (2019).

[4] M. A. Richards, J. A. Scheer, and W. A. Holm, Principles of Modern Radar: Basic Principles. Scitech Publishing, Edison, New Jersey (2010)

[5] A. S. Bahri, Supriyanto, and B. J. Sentosa, Penentuan Karakteristik Dinding Gua Seropan Gunungkidul dengan Metode Ground Penetrating Radar, Institut Teknologi Sepuluh Nopember, Surabaya (2018)

[6] K. Pentoś, D. Łuczycka, and T. Wysoczański, Dielectric Properties of Selected Wood Species in Poland, Wroclaw University of Environmental and Life Sciences, Poland (2017)

[7] A. Fuchs, M. J. Moser, H. Zangl, and T. Bretterklieber, Using Capacitive Sensing to Determine The Moisture Content Of Wood Pellets – Investigations and Application, *International Journal On Smart Sensing And Intelligent Systems*, (2009)

[8] W. A. Nuraini, Analisis Hubungan Kadar Air Kerupuk dengan Permitivitas Relatif dan Simulasi Desain Sensor untuk Menentukan Distribusi Kadar Air, *Food and Agriculture Organization of the United Nations,* (2016)

[9] Nosherwan Shoaib, Vector Network Analyzer (VNA) Measurements and Uncertainty Assessment, *Springer*, Cham (2017)

[10] A. A. Pramudita, T. O. Praktika, and S. Jannah, Radar Modeling Experiment Using Vector Network Analyzer, *2020 International Symposium on Antennas and Propagation* (ISAP), (2021), 99-100.

[11] D. A. B. Báez-López, José Miguel David and Villegas, MATLAB Handbook with Applications to Mathematics, Science, Engineering, and Finance, CRC Press, Boca Raton, Florida (2019)

[12] Dr. Brijesh Bakariya and Dr. Kulwinder Singh Parmar, Fundamental Concepts of MATLAB Programming From Learning the Basics to Solving a Problem with MATLAB, BPB Publications, India (2020)

[13] S. Selladurai, Ultrasonic Scanning Methods A, B and C Scan Displays, in Engineering Physics Part I, Asoke K. Ghosh, *PHI Learning Private Limited*, New Delhi (2010) 10–11.

[14] Sumariyah, Z. Muchlisin, and E. Setiawati, Rekontruksi Citra Tomografi Sinar-X Flouresens 2D Berbasis Teknik Radiografi Digital Menggunakan Bahasa Pemrograman Matlab 7.1, *Berkala Fisika*, 13(4) (2010), 133–138.

[15] A. N. Kurniawan, T. S. Widodo, and I. Soesanti, Penapisan Artifak Logam pada Citra CT-scan dengan Spatial Filter, *JNTETI*, 2(4) (2013)

[16] Santoso, H. Hutapea, and K. Aris, Analisis Pengujian S-Parameter pada Perangkat Duplexer dan Kabel Coaxial dengan Frekuensi 1.800 Mhz, *Jurnal Teknik dan Ilmu Komputer*, (2017).

[17] P. Seldi, Pengaruh Durasi Perlakukan Panas dengan Minyak (*Oil Heat Treatment*) Terhadap Perubahan Sifat Fisis dan Mekanis Kayu Akasia (*Acacia Mangium*) dan Kayu Jabon (*Anthocephalus Cadamba*), Universitas Lampung, Lampung (2020)

[18] A. Somantri, A. Pulung dan I. Mimin, Aplikasi Metode Ground Penetrating Radar terhadap Pola Retakan di Bendungan Batu Tegi Lampung, *Wahana Fisika,* Universitas Pendidikan Indonesia, Bandung (2016)

[19] R. Seal and J. Urbina, GnuRadar: An Open-Source Software-Defined Radio Receiver Platform for Radar Applications, *IEEE Aerospace and Electronic Systems Magazine.*, 35(2) (2020), 30-36

[20] B. Bleszynski, A simple radar based on USRP software defined radio, *2017 Signal Processing Symposium (SPSympo)*, Jachranka (2017)

Author information

Aldi Rivaldi Dwinanda was born in Bandung, in 2000. He received the bachelor degree in telecommunication engineering from Telkom University, Indonesia in 2022. He is interested in radar topics and one of the radar laboratory assistant.

Bambang Setia Nugroho obtained a bachelor's degree in 1999 and master's degree in 2004, both of which were from the Bandung Institute of Technology (institute Teknologi Bandung – ITB), Indonesia. In 2015, he obtained a PhD in Electrical Engineering from the University of Indonesia. Currently, he works as a lecturer in the School of Electrical Engineering, Telkom University, Indonesia. His research interest includes microwave technology, antenna engineering, electromagnetics, by which he has been publishing journal articles in various international proceedings and national

journals. Besides, he is an active reviewer at international telecommunication conferences.

Aloysius Adya Pramudita
(S'08 M'12) was born in Klaten, Indonesia, in 1977. He received the B.S. in electrical engineering from Gadjah Mada University, Indonesia in 2000, M.S. and Ph.D degree in electrical engineering from the Bandung Institute of Technology, Indonesia in 2005 and 2009 respectively. From 2002 to 2016, he was a Lecturer and Researcher with the Atma Jaya Catholic University, Indonesia. From 2013 to 2016, He was head of Electrical Engineering Department of Atma Jaya Univeristy and from 2016 to 2017 as head of Electrical Engineering Graduate Program of Atma Jaya Catholic University. Since 2017, he joined the Telecommunication Engineering Department of Telkom University, Bandung, Indonesia. He responsible as head of Satellite Communication and Radar Laboratory of Telkom University. He also serves as a reviewer for several technical journals and conferences in his interest area. His research interests include antenna theory and design for telecommunication and radar, electromagnetics and wave application, and radar system for contactless sensor.

Open Access Policy